CHARACTERIZATION AND MODELING FOR DILUTE AND DENSE SPRAYS

C.P. Chen, Y.M. Kim, and H.M. Shang
University of Alabama in Huntsville
Huntsville, Alabama

Abstract

This study involves the development of numerical modelling in dilute and dense spray combustion. The governing gas-phase equations in Eulerian coordinate are solved by a time-marching multiple pressure correction procedure based on the operator-splitting technique. The droplet-phase equations in Lagrangian coordinate are solved by a stochastic discrete droplet technique. The $k-\epsilon$ model is used to characterize the time and length scales of the gas phase turbulence for droplet dispersions and droplet/turbulence interactions. To account for the dense spray effects, an existing drop collision and coalescence model and a Taylor analogy breakup(TAB) model are employed. These models are incorporated into a state-of-the-art multiphase all-speed transient flow solution procedure. A sequence of validation cases involving non-evaporating, evaporating, burning, dilute and dense spray cases are included. In the combusting dilute spray case, the present numerical procedure correctly predicts the general features of spray-combustion flows and yields the qualitative agreement with experimental data. The discrepancies observed in the results are attributed mainly to uncertainties in the initial spray distributions and the droplet/wall model, the single-step fast chemistry employed by the combustion model, and the deficiencies of the $k-\epsilon$ turbulence model dealing with the strong streamline curvature. For non-evaporating, evaporating, and burning dense spray cases, the predictions show a reasonably good agreement with available experimental results in terms of spray penetration, drop size distributions, and overall characteristics of the evaporating and burning spray.

I. Introduction

There have been a number of research efforts[1-6] towards the development of numerical and physical models for spray combustion. Many aspects of sprays including fuel properties of droplets [1], multicomponent nature of fuel [2], evaporation models [3] have been studied and excellent reviews on analysis and measurements of sprays have also been given in Refs. [4,5,6]. These studies are motivated by the need for better understanding of multi-phase turbulent combustion processes as well as the demand for improving performance, stability, and emission control in industrial furnaces and propulsive systems such as gas turbine, ramjet engines, and space shuttle main engines.

The prediction of the local flow properties of spray flames requires the solutions of multi-phase dynamics, and accounts for complex interactions between the dispersed droplets and the continuous gas-phase flows. Various approaches have been suggested to model the interphase transport phenomena. The methodologies for the spray combustion computations are largely classified as the discrete droplet model, the statistical droplet model, and the two-fluid continuum model. Comparative performances for three approaches are well summarized in Ref.[6]. Among three models, the discrete droplet model has gained wide acceptance due to its computaional efficiency, the flexibility in handling poly-disperse spray, the convenient interphase coupling, and the elimination of numerical diffusion. With Eulerian-Lagrangian formulations in multi-phase flows, the stochastic separated flow(SSF) approach[5] categorized in the discrete droplet model is usually employed to account for the turbulence effects on interphase transport. In the present stochastic separated flow model, the mathematical formulation of the two-phase flow and combustion processes comprises the Eulerian conservation equation for the gas phase and the Lagrangian equations for the fuel droplets. The link between two phases is mathematically expressed in terms of liquid/gas-phase interaction source terms in the gas-phase equations. The governing gas-phase equations in Eulerian coordinate are solved by a time-marching multiple pressure correction procedure based on the operator-splitting technique. The droplet-phase equations in Lagrangian coordinate are solved by a stochastic discrete droplet technique. The $k-\epsilon$ model is used to characterize the time and length scales of the gas phase turbulence for droplet dispersions and droplet/turbulence interactions. The present vaporization model includes the effects of variable thermophysical properties, non-unitary Lewis number in the gas-film, the Stefan flow effect, and the effect of internal circulation and transient liquid heating.

In the dilute spray combustion models, the stochastic separated flow model is employed to account for the turbulent droplet dispersion, turbulence is represented by the $k-\epsilon$ model, and the combustion processes involves an irreversible one-step reaction at an infinite rate. The turbulent fluctuations on the mixture properties are introduced by the probability density function(pdf) approach. The centrifugal force terms associated with the swirl effects are also included in the gas-phase/droplet-phase equations. In the study, we evaluate the solution procedure and the physical submodels of turbulence, combustion, vaporization, swirling effects, and initial spray distributions. The

present numerical model for the multi-phase turbulent reacting flows has been tested by applying it to predict the local flow properties in two axisymmetric, confined, swirling spray-combusting flows[32]. Special emphasis is given to the influence of the spray initial conditions and the inlet swirl strength which characterize the spray vaporization and the turbulent mixing. Two swirl numbers are considered to investigate the influence of swirl on the droplet evaporation and trajectories, and the effects of droplet/ turbulence interactions in flow properties. The predictive capabilities of the present procedure have been demonstrated by comparisons with experimental data. The present numerical procedure correctly predicts the general features of spray-combustion flows and yields the qualitative agreement with experimental data. However, quantitative differences exist especially at near-burner locations, at near-wall regions, and along the combustion chamber centerline. The discrepancies observed in the results are attributed mainly to uncertainties in the initial spray size and velocity distributions and the droplet/wall impingement interaction, the single-step fast chemistry employed by the combustion model, and the deficiencies of the $k-\epsilon$ turbulence model dealing with the strong streamline curvature.

One of the important aspects in spray combustion modeling is the dense spray effects which include atomization process, drop breakup, droplet collision and coalescence. Atomization process occurs on time and length scale too short to be resolved with practical computation grid sizes and time steps. Thus, atomization should be modeled as a sub-grid-scale process. To account for the dense spray effects, the present study employs the drop collision & coalescence model[8] and the Taylor analogy breakup(TAB) model[9]. In the drop collision model, the probability distributions governing the number and outcomes of the collisions between two drops are sampled randomly in consistency with the stochastic particle tracking method. The TAB model utilizes an analogy between an oscillating and distorting droplet and a spring-mass system. The present breakup model is based on the reasonable assumption that atomization and drop breakup are indistinguishable processes within a dense spray near the nozzle exit. Accordingly, atomiztion is prescribed by injecting drops which have a characteristic size equal to the nozzle exit diameter. Compared to Reitz's model[31], the TAB model has several advantages in terms of no need to input the spray angle, an easy introduction of liquid viscosity effects, and explicit informations of distortion and oscillation effects on the interphase exchange rates of mass, momentum, and energy. For non-evaporating, evaporating, and burning dense spray cases, the predictions show a reasonably good agreement with available experimental results in terms of spray penetration, drop size distributions, and overall characteristics of the evaporating and burning spray.

II. Physical and numerical models

All the gas- phase and liquid-phase processes are modeled by a system of unsteady, two-dimensional (axisymmetric) equations. The gas-phase equation is written in Eulerian coordinate whereas the liquid-phase is presented in Lagrangian coordinates. The two-way coupling between the two phases is described by the exchange rate terms which represent the rates of momentum, mass and heat transfer. These equations are given below.

Gas-Phase Equations

The density-weighted conservation equation of mass, momentum, and scalar variables in Eulerian coordinate can be written as follows:

$$\frac{\partial \rho}{\partial t}+\frac{\partial}{\partial x_i}(\rho U_i)=S^m{}_l \tag{1}$$

$$\frac{\partial \rho U_i}{\partial t}+\frac{\partial}{\partial x_j}(\rho U_i U_j)=-\frac{\partial P}{\partial x_i}-\frac{\partial}{\partial x_j}[\rho\overline{u_i' u_j'}]+S^i{}_l \tag{2}$$

$$\frac{\partial \rho \Theta}{\partial t}+\frac{\partial}{\partial x_i}(\rho U_i \Theta)=-\frac{\partial}{\partial x_i}[\rho\overline{u_i'\theta'}]+S^\Theta{}_g+S^\Theta{}_l \tag{3}$$

where ρ is the time-mean density of the mixture, U_i and u_i' are the i component of the density-weighted mean and fluctuating part of the instantaneous velocity, Θ and θ' are the density-weighted mean and fluctuating part of an instantaneous scalar quantities including the species concentrations and the internal energy, P is the mean pressure, S_g and S_l represents the gas-phase source terms and the interaction source terms due to the fuel spray, respectively. Detailed expressions for these source terms can be found in Ref. [10,11]. To close the system of equations, we need to model the unknown correlations, $\overline{u_i'u_j'}$ and $\overline{u_i'\theta'}$.

Turbulence Models

The two-equation effective diffusivity model is used to represent the turbulent characteristics. In the eddy diffusivity models, the turbulent fluxes, $\overline{u_i'u_j'}$ and $\overline{u_i'\theta'}$, are related to the mean flow gradients through the assumption of an isotropic eddy viscosity and a constant turbulent Prandtl or Schmidt number:

$$\rho\overline{u_i'u_j'}=-\mu_t\left(\frac{\partial U_i}{\partial x_j}+\frac{\partial U_j}{\partial x_i}\right)+\frac{2}{3}\delta_{ij}\left(\rho k+\mu_t\frac{\partial U_k}{\partial x_k}\right) \tag{4}$$

$$\rho\overline{u_i'\theta'}=-\frac{\mu_t}{\sigma_t}\left(\frac{\partial \Theta}{\partial x_j}\right) \tag{5}$$

The eddy viscosity(μ_t) appearing in (4) and (5) is defined in terms of a characteristic turbulence length scale($k^{3/2}/\epsilon$) and a velocity scale ($k^{1/2}$), so that μ_t is given by

$$\mu_t=C_\mu\rho\frac{k^2}{\epsilon} \tag{6}$$

The turbulent kinetic energy, k, and its dissipation rate, ϵ, can be modeled from the turbulent transport equations:

$$\frac{\partial \rho k}{\partial t}+\frac{\partial}{\partial x_j}(\rho U_j k)=\frac{\partial}{\partial x_j}\left(\mu+\frac{\mu_t}{\sigma_k}\right)\frac{\partial k}{\partial x_j}-\rho\overline{u_i'u_j'}\frac{\partial U_j}{\partial x_j}$$

$$-\frac{\mu_t}{\rho^2}\frac{\partial \rho}{\partial x_j}\frac{\partial P}{\partial x_j}-\rho\epsilon \tag{7}$$

$$\frac{\partial \rho\epsilon}{\partial t} + \frac{\partial}{\partial x_j}(\rho U_j \epsilon) = \frac{\partial}{\partial x_j}(\mu + \frac{\mu_t}{\sigma_\epsilon})\frac{\partial \epsilon}{\partial x_j} + C_{\epsilon 1}\frac{\epsilon}{k}(\rho\overline{u_i' u_j'}\frac{\partial U_j}{\partial x_j}$$

$$+\frac{\mu_t}{\rho^2}\frac{\partial \rho}{\partial x_j}\frac{\partial P}{\partial x_j}) - C_{\epsilon 2}\rho\frac{\epsilon^2}{k} \quad (8)$$

Here, terms involving $\frac{\partial \rho}{\partial x_j}$ in (7) and (8) are inserted to account for variable-density effects [12]. These terms originally come from the pressure-velocity correlation in the Reynolds stress equation. For reacting flows, these terms should account partially for the expansion effect on the flow field due to heat release from combustion.

Combustion Model

It is assumed that the spray is dilute and the liquid fuel droplets act as distributed sources of fuel which evaporate to form a cloud of vapour. This implies that combustion process in spray flames can be treated as turbulent gaseous diffusion flames. Experimental evidence for this assumption can be found in Ref.[13]. An idealized approach for physically-controlled diffusion flames is to invoke a fast-chemistry assumption which the chemistry is sufficiently fast and intermediate species do not play a significant role. In the turbulent diffusion flame model, the influence of turbulence on combustion is taken into account by relating the fluctuations of mass fractions. This implies that fuel and oxidizer can coexist in the same place but at a different time. The most convenient way to include the effect of turbulent eddies on thermochemical properties is via the introduction of the probability density function(pdf), $P(\xi, x_i)$. This function contains information of both mean(f) and variance of $(g = (f - \overline{f})^2)$ of the mixture fraction. These variables f and g can be obtained by solving the transport equations. The density-weighted mean values($\overline{\phi}$) of any property are evaluated by convoluting the property functions with a probability density fuction, $P(\xi, x_i)$:

$$\overline{\phi} = \int \phi(\xi) P(\xi, x_i) d\xi \quad (9)$$

Numerous probability density functions are available in the literatures. The present study adopts the β-pdf which is known as the widely applicable one [12]. A modified eddy breakup model[14] is optionally incorporated in the present computer code. This model is used for the prediction of the transient spray-combusting flows.

Droplet-Phase Equations

The two-phase interactions are particularily important for pressure atomized injectors, where a significant proportion of the initial momentum in the flow is carried by the liquid phase and is transfered to the gas phase only by the drag force on droplets. Droplet life histories are needed to determine the source terms arising from the interaction between the gas and the droplets. Mean gas-phase properties and instantaneous eddy properties are used for the stochastic droplet tracking calculations. The droplet evaporation rates are given by the Frossling correlation [16] and the transient droplet temperatures are obtained by the infinity conductivity model[17]. The major assumptions and the detailed formulations in the droplet transport calculations can be found in Refs.[4,5,17]. The correct evaluation of the average physical propertites in the gas film is of importance in the vaporation calculations. In accordance with the Hubbard et al. [18] recommendations, the 1/3 rule has been used in the present study. The variable thermophysical properties such as the fuel vapour pressure are estimated from the JANAF data bank[19]

Turbulence/Droplet Interactions

The situation to be considered in this study is the dilute dispersed flows in which drop collisions are infrequent and mass, heat transfer and drags of individual drops are not directly influenced by adjacent droplets. The two-way coupling between gas and droplets involves interactions at mean flowfield and interactions at fluctuation levels in turbulent flows. Major issues in turbulence/droplet interactions include the turbulent dispersion of the dispersed phase, turbulence modulation effects due to droplets, and the effect of turbulence on interphase transport rates.

In this study, the turbulence effects on droplet dispersion are simulated by a Monte Carlo method in the sense that a fluctuating velocity u_i', where each component of u_i' is randomly chosen from a Gaussian distribution with standard deviation $\sqrt{\frac{2}{3}k}$, is added to the mean gas velocity. Thus the turbulence is assumed to be isotropic. This type of simulation for the turbulent dispersion of droplets has been extensively used previously [20,21,22] for statistically stationary turbulent dispersed flows. Main differences in the implementations are the methods used to specify turbulence eddy properties and the methods for choosing the time of interaction of a particle with a particular eddy. The details of simulation procedures and also of various aspects associated with the interaction times can be found in Ref. [11].

Drop Breakup and Collision

The present study employs the TAB (Taylor Analogy Breakup) model proposed by O'Rourke and Amsden[9]. This model is based on an analogy between an oscillating and distorting droplet and a spring-mass system. The restoring force of the spring is analogous to the suface tension forces. The external force on the mass is analogous to the gas aerodynamic force. The damping forces due to liquid viscosity are introduced to this analogy. Compared to Reitz's model[31], the TAB model has several advantages in terms of no need to input the spray angle, an easy introduction of liquid viscosity effects, and the explicit informations of distortion and oscillation effects on the interphase exchange rates of mass, momentum, and energy. The major limitation of the TAB method is that only one oscillation mode can be tracked. However, in reality there exist many such modes in the Taylor analogy. Despite this limitation, good agreement between numerical results and experimentally observed bag/stripping breakup times has been reported. The droplet oscillation & breakup calculations require two normalized particle arrays(deformation and oscillation) which can be determined by the equation for the acceleration of the droplet distortion parameter. Occurance

of droplet breakup, the Sauter mean radius(SMR), and oscillation velocity for the product drop depend on these two parameters and Weber number. The radius of the product drops is then chosen randomly from a chi-squared distribution with calculated SMR. Following breakup, the product drop has the same temperature with the parent drop, and its deformation and oscillating parameters are set to zero.

The drop collision model suggested by O'Rourke[8] is employed to calculate collision and coalescence among the dispersed liquid phase. The collision routine is operating-ing for the pair of particles if, and only if, they are in the same computational cell. For the collision calculation, the drops associated with each computation parcel are considered to be uniformly distributed throughout the computational cell where they are located. For all parcels in each computational cell, a collision frequency between drops between the parcel($parcel_1$) of larger drop radius(r_1) and the parcel($parcel_2$) of smaller drop radius(r_2) is obtained from the relationship in terms of the number of drops in $parcel_2$, the relative velocity between $parcel_1$ and $parcel_2$, the area based on r_1+r_2, and the volume of computational cell. The probability with n collisions is assumed to follow a Poisson distribution based on a collision frequency and the computational time step. Using the probability informations, the collision impact parameters are stochastically calculated. If the collision impact parameter is less than a critical impact parameter, the outcome of every collision is coalescence. In opposite case, each collision is a grazing collision. The critical impact parameter depends on the drop radii, the relative velocity between drops, and the liquid surface tension coefficient.

Droplet/Wall Impingement

The wall impingement model adopts the jet treatment[33] and the empirical correlation approach[34]. The experimental data of Wachters and Westerling[35] can be numerically fitted in terms of the droplet Weber number before impact and after impact.

$$We_o = 0.678 We_i e^{(-0.004415 We_i)} \tag{10}$$

For $We_i \leq 80.0$, the drops do not disintegrate during impact and bounce from the surface while for $We_i > 80.0$, the disintegration produced a dispersion of the small drops on the surface. Thus, in case of $We_i > 80.0$, the jet model is used;in case of $We_i \leq 80.0$, the drops bounces from the surface and the normal velocity after impact can be calculated from the following equation.

$$V_o = V_i (We_o/We_i)^{0.5} \tag{11}$$

This wall impingement model is based on several assumptions such as extrapolation of the results with water drops at atmospheric conditions and at higher wall temperature, no breakup at impact, the neglect of the wall heat transfer, and the neglect of droplet interaction with a possible liquid wall film. Despite these limitations, the qualitative agreement for $We_i \leq 80.0$ and the good quantitative agreement for $We_i > 80.0$ have been reported.

Numerical Procedure

The present method is based on the operator splitting technique[23] attempting to reach accurate transient solution after prescribed predictor- corrector steps for each time-marching step. The previous multiple pressure-correction method[11.27] is extended to to handle the strong nonlinear couplings arising in the multi-phase, fast-transient, and reacting flows. This method is non-iterative and applicable to all-speed flows. The additional scalar conservation equations such as species, and enery are incorporated into the same predictor-corrector sequence. Discretization of the gas phase governing equation uses the finite volume approach. To enhance the numerical stability, the implicit Euler scheme is employed in differencing the temporal domain. All the dependent and independent variables are stored at the same grid location and the variables at the finite control volume boundaries are interpolated between adjacent grid points. The discretizations have been performed on a general non-orthogonal curvilinear coordinate system with a second order upwind scheme for convection terms and the central differencing scheme for diffusion terms. The resulting discretized equations were solved by a conjugate gradient (CGS) solver. In the present algorithm, each time step is divided into a one-predictor/two-corrector sequence. The strong coupling terms between particle and gas are evaluated by the same time splitting technique. Implicit coupling procedures are used to treat momentum exchanges to avoid the small timesteps. The unsteady solution procedure described above is somewhat different from the conventional PSIC(particle source in cell) procedure[25] in which global iterations are required. The method used here is non-iterative and time-accurate.

III. Results and discussions

Evaporating and burning dilute spray

The present numerical model for the multi-phase turbulent reacting flows has been tested by applying it to predict the local flow properties in two axisymmetric, confined, swirling spray-combusting flows[32]. The combustor geometry of the second test case is shown in Fig. 1. Experimental data for temperature, axial and tangential velocity components were obtained from measurement of Khalil et. al.[32]. The inlet conditions and the initial droplet size distribution are given in Table 1. Liquid kerosene was used as fuel and the air/fuel mass ratio was fixed at 20.17.

In the present study, two swirling numbers(S=0.72 and 1.98) were considered to investigate the influence of swirl on the droplet evaporation & burning characteristics. Fig. 2-4 show the general flow pattern such as the predicted droplet trajectories, velocity vectors, and temperature contours of two swirl cases. In the lower swirl case(S=0.72), large portion of droplets survive in the central recirculation zone and continue to evaporate in the far downstream region. In the high swirl case(S=1.98), most of small droplets are trapped in the recirculation zone and evaporate there, producing intensive burning and high temperature in this region. With increasing swirl, the droplet spreading in-

creases due to the droplet dispersion and the increased particle centrifugal force term. In addition, the larger central recirculation zone corresponding to the higher inlet swirl is contributed to recirculate more hot combustion gas from downstream and to increase the temperature at near inlet regions.

The predicted and measured temperature profiles for two swirl cases are shown in Fig. 5 and 6. Both the measurements and the prediction show the high- temperature peaks near the downstream combustor wall where droplets have traversed and evaporated. The discrepancies in near-wall regions partly result from the uncertainties of droplet/wall impingement process. However, the deviations in other locations are associated with the deficiencies of turbulence and combustion models, the unreliable informations of the inlet droplet size & velocity distribution, and the potential errors in inlet swirl profiles and inlet turbulence length scale. It is observed that the temperature profiles of the high swirl case are more uniform than those of the low swirl case. Radial profiles of axial velocity velocity for S=0.72 and 1.98 are shown in Fig. 7 and 8. The present numerical model underpredicts the magnitude of the reverse flow velocities. The poor performance of the present numerical model in predicting the size of central recirculation zone and the reverse velocity is partly attributed to the deficiency of $k-\epsilon$ model based on the isotropic assumption. The predicted and measured tangential velocities for two swirl cases are presented in Fig. 9 and 10. The significant deviation close to the inlet is likely caused by the incorrect distribution of inlet swirl velocities. In the present study, the inlet swirl velocities are obtained from the estimated axial angular momentum flux. The rapid decay of the tangential velocity to the solid body rotation close to the centerline could be tied with the errors in the prediction of reverse velocities.

Non-evaporating solid-cone dense spray

The solid-cone spray measurements of Hiroyasu and Kadato[28] were used to validate the present numerical dense spray model which includes collison, coalescence, and breakup models described above. Liquid fuel is injected through a single hole nozzle into constant pressure, room-temperature nitrogen. Spray tip penetration and drop sizes were measured from photographs of the backlighted spray. The test conditions are given in Table 2 (SMD is the average over the spray cross-section 65 mm downstream of the nozzle). The nozzle diameter was 0.3 mm and the present computations used tetradecane for the liquid fuel(the experiments used a diesel fuel oil with physical properties close to tetradecane).

A computational domain of 20 mm in radius and 120 mm in length was discretized by a 25 radial and 45 axial grid. The mesh spacing was nonuniform with refinement on the centerline and close to the injector. The smallest cell is 0.5 mm radially and 1.5 mm axially. Since this dense spray calculation is sensitive to the grid resolution, the fine grid was used to obtain a grid-independent solution. The number of computational parcels at steady-state conditions was between 1000 and 1500, and the number was varied with the back pressure. The present numerical results did not change appreciably when this parcel number was varied. The initial turbulent quantities were assumed as the small values(k = 1 x $10^{-3} m^2/s^2, \epsilon$ = 4 x $10^{-4} m^2/s^3$). The numerical results were insensitive to these initial values.

The spray parcel distribution for three sprays is shown in Figure 11. This plot indicates that the spray tip penetration and the core length decrease with the increase of the gas density. Figure 12 shows the predicted and measured spray tip penetration versus time. It can be seen that there is reasonably good agreement between the prediction and the measurement . In the present computations, the spray tip was defined to be the location of the leading spray drop parcel. It is necessary to note that a far-field spray penetration is not a sensitive indicator of model performance. Previous studies[26,29] indicated that a far-field spray penetration is mostly influenced by the turbulence diffusivity. However, a near-field spray penetration could be more sensitive to the physical submodels such as breakup and collision. Figure 13 shows the variation of SMD with axial distance from the injector. The three solid data at 65 mm correspond to the measurements. The computed drop size is a time average over the spray cross-section at each axial location. At the nozzle exit, the drop diameter is equal to the nozzle diameter, 0.3 mm. Generally these curves can be broken into two sections. Close to the injector, the drop size decreases rapidly due to drop breakup. Further downstream, the drop size increases gradually due to drop coalescence. In the low gas pressure case(1.1 MPa), the drop size remains relatively uniform after initial breakup region and then increases slightly in the far-downstream region. For the high pressure cases(3.0 and 5.0 MPa), the drop size increases largely in far-downstream region, because higher gas densities promote collisions and coalescence. This trend is also observed in the measuments. The predicted drop sizes at 65 mm are qualitatively agreed with the experimental data for all three cases. The discrepancy could be associated to the fact that the experimental sprays were pulsed while the computations assumed a constant pressure injection for the entire computational time period.

Evaporating and burning solid-cone dense spray

The evaporating and buring solid-cone spray measurement of Yokoda et. al.[30] have been used to validate the present numerical dense spray model. Liquid fuel(tridecane) is injected through a sigle hole nozzle into high-pressure, high-temperature nitrogen or air. The test conditions for evaporating and burning sprays are given in Table 3. The nozzle diameter was 0.16 mm. A computational domain of 20 mm in radius and 100 mm in length was discretized by a 21 radial and 44 axial grid. The mesh spacing was nonuniform with refinement on the centerline and close to the injector. The number of computational parcels at steady-state conditions was between 500 and 700. Due to the numerical reasons, the initial turbulent quantities were assumed as the small values. The upstream boundary is treated as a solid wall, and other boundary are treated as open boundaries.

Figure 14 shows the spray parcel distribution and the contours of the fuel mass fraction for evaporating sprays. These results show that the spray penetration increase with

respect to time at early period of injection, however the penetration become nearly constant after $t = 0.2ms$ due to evaporation. Even though the liquid drop does not penetrate more, the evaporated fuel vapor continuously penetrate with respect to time. Comparisons of the computed and experimental spray penetration versus time are shown in Figure 15. The present spray penetration distance agrees well with the measured results[30]. Figure 16 and 17 shows the spray parcel distribution, the contours of the fuel mass fraction, temperature, and oxygen mass fraction at different times of injection for burning sprays. The computed configuration of a burning spray flame has the overall agreement with the measure ones. In the experimental study, a considerable level of soot was observed near the spray tip where the equivalence ratio is low and the temperature is high due to the progressed turbulent mixing. Therefore, the soot model should be incorporated to improve the prediction capability of the present burning dense spray model. Future studies may include the detailed comparison with the local properties available in the experiment.

IV. Summaries

The numerical models have been developed for the analysis of dilute and dense spray-combusting flows. A numerical model for the prediction of the statistically stationary spray- combusting flows is evaluated by comparison with the available experimental data. The present numerical procedure correctly predicts the general features of spray-combustion flows and yields the qualitative agreement with experimental data. However, quantitative differences exist especially at near-burner locations, at near-wall regions, and along the combustion chamber centerline. The discrepancies observed in the results are attributed mainly to uncertainties in the initial spray size and velocity distributions and the droplet/wall impingement interaction, the single-step fast chemistry employed by the combustion model, and the deficiencies of the $k - \epsilon$ turbulence model dealing with the strong streamline curvature. To improve the prediction capabilities of the present numerical procedure, the future works must include the consistent studies of non-evaporating, evaporating, and burning sprays by utilizing the non-isotropic turbulence model such as the algebraic stress model and the second-moment closures, and the multi-step finite chemistry model.

For non-evaporating, evaporating, and burning dense spray cases, the predictions show a reasonably good agreement with available experimental results in terms of spray penetration, drop sizes, and overall configuration of a burning-spray flame. To improve the prediction capabilities and efficiencies of the numerical and physical models, future works must include the extensions of the dispersion width transport model to non-evaporating, evaporating, and burning dense sprays, the incorporation of supercritical vaporization model, the incorporation of soot model and further refinement of atomization and breakup models.

Acknowledgements

The current work is done under the support of NASA grant NAG8-092 and NASA contract NAS8-36955.

References

1. Asheim, J.P. and Peters, J.E.(1989), "Alternative Fuel Spray Behavior", *J. Propulsion and Power*, **5**, pp. 391-398.
2. Aggarwal, S.K.(1988), "Ignition Behavior of a Dilute Vaporizing Multicomponent Fuel Spray", AIAA-88-0635, 26th Aerospace Sciences Meeting, Reno, Nevada, Jan.
3. Sirignano, W.A.(1983), "Fuel Droplet Vaporization and Spray Combustion" , *Prog. Energy Comb. Sci.*, **9**, pp. 291-322.
4. Law, C.K.(1982), "Recent Advances in Droplet Vaporization and Combustion", *Prog. Energy Comb. Sci.*, 8, pp. 171-201.
5. Faeth, G.M.(1987), "Mixing, Transport and Combustion in Spray", *Prog. Energy Comb. Sci.*, **13**, pp. 293-345.
6. Sirignano, W.A.(1986), "The Formulation of Combustion Models: resolution compared to droplet spacing," *ASME Journal of Heat Transfer*, **108**, pp. 633-639.
7. Litchford, R.J. and Jeng, S.M.(1991), "Efficient Statistical Transport Model for Turbulent Particle Dispersion in Sprays", *AIAA J.*, **29**, no. 9, pp. 1443-1451.
8. O'Rourke, P.J.(1981) "Collective Drop Effects on Vaporing Liquid Sprays", Los Alamos National Laboratory report LA-9069-T.
9. O'Rourke, P.J.(1987), "The TAB Method for Numerical Calculation of Spray Droplet Breakup", SAE Technical Paper 872089.
10. El Banhawy, Y., and Whitelaw, J.M.(1980), "Calculation of the Flow Properties of a Confined Kerosene-Spray Flames", *AIAA J.*, **18**, pp. 1503-1510.
11. Kim, Y.M., Shang, H.M., and Chen, C.P.(1991), "Non-Isotropic Turbulence Effects on Spray Combustion", AIAA Paper 91-2196, 27th Joint Propulsion Conference, Sacramento, CA, June 24-26.
12. Jones, W.P.(1980), "Models for Turbulent Flows with Variable Density and Combustion", in W. Kollman (ed.), Prediction Method for Turbulent Flows, Hemisphere Publishing, London, pp. 379-422.
13. Tuttle, J.H., Shisler, R.A., and Mellor, A.M.(1976), "Investigation of Liquid Fueled Turbulent Diffusion Flames", *Combustion Science and Technology*, **14**, pp. 229-241.
14. Magnussen, B.F. and Hjertager, B.H.(1977), "On Mathematical Modeling of Turbulent Combustion With Special Emphasis on Soot Formation and Combuation", 16^{th} Symposium on Combustion, p. 719.
15. Westbrook, C.K. and Dryer, F.L.(1984), "Chemical Kinetic Modelling of Hydrocarbon Combustion," *Prog. Energy Comb, Sci.*, Vol.10, pp. 1-57.
16. Frossing, N.(1938), "On the Evaporation of Falling Droplets", *Gerlands Beltrage Zur Geophysik*, **52**, pp. 170-216.

17. Abramzon, B. and Sirignano(1988), "Droplet vaporization model for spray combustion calculations," AIAA Paper 88-0636, 26th Aerospace Science Meeting, Reno, Nevada.

18. Hubbard, G.L. et al.(1975), "Droplet Vaporization : Effects of Transient and Variable Properties", *Int. J. Heat and Mass Transfer*, **18**, pp. 1003- 1008.

19. Stull D.R. and Prophet H.(1974), "JANAF Thermochemical Table", 2nd edition, N.W. Chase et al., *J. Phys. Chem. Ref. Data*, **3**, 311.

20. Gosman, A.D. and Ioannides, E.(1981), "Aspects of Computer Simulation of Liquid Fueled Combustors", AIAA 81-0323.

21. Fashola, A. and Chen, C.P.(1990), "Modeling of Confined Turbulent Fluid- Particle Flows Using Eulerian and Lagrangian Schemes", *Int. J. Heat and Mass Transfer*, **33**, pp. 691-700.

22. Shuen, J.S. et al(1985). "Structure of Particle-Laden Jets : Measurements and Predictions", *AIAA J.*, **23**, pp. 396-404.

23. Issa, R.I.(1985), "Solutions of the Implicitly Discretized Fluid Flow Equations by Operator Splitting", *J. Comp. Physics*, **62**, pp. 40-65.

24. O'Rourke, P.J.(1989), "Statistical Properties and Numerical Implementation of a Model for Droplet Dispersion in a Turbulent Gas", *J. Comp. Physics*, **83**, pp. 345-360.

25. Crowe, C.T., Sharma, M.P. and Stock, D.E.(1977), "The Particle Source in Cell Method for Gas-Droplet Flows", *J. Fluid Eng.* **99**, pp. 325-332.

26. Chen, C.P., Shang, H.M. and Jiang, Y.(1990), "A Novel Gas-Droplet Numerical Method for Spray Combustion", Eigth Liquid Rocket Engine CFD Working Group Meeting, NASA-MSFC, April 17-19, 1990, to be appeared in the *Int. J. Numer. Meth. Fluids*, 1992.

27. Chen, C.P., Jiang, Y., Kim, Y.M., and Shang, H.M.(1991) "MAST - A Multi-Phase All-Speed Transient Navier-Stokes Code in Generalized Coordinates", NASA Contract Report, NAG8 -092, Dec., 1991

28. Hiroyasu, H. and Kadato, T.(1974), "Fuel Droplet Size Distribution in Diesel Combustion Chamber," SAE Paper 740715.

29. Dukowicz, J.K.(1980), "A Particle-Fluid Numerical Model for Liquid Sprays", J. Comp. Physics, 35, pp. 229-253.

30. Yokota, H., Kamimoto, T., and Kobayashi, H.(1988), "A Study of Diesel Spray and Flame by an Image Processing Technique, *Bulletin of JSME*, **54**, p. 741.

31. Reitz, R.D. and Diwaker, R.(1987), "Structure of High Pressure Fuel Sprays," SAE Paper 870598, 1987

32. Khalil, K.H., El-Mahallawy, F.M., and Moneib, H.A., "Effect of Combustion Air Swirl on the Flow Pattern in a Cylindrical Oil Fired Furnace", Sixteenth Symposium on Combustion, The Combustion Institute, Pittsburgh, PA, pp. 135-143, 1977

33. Gonzalez, M.A. and Reitz, R.D.(1991), A Study of Diesel Cold Starting using both Cycle Analysis and Multidimensional Calculations", SAE Technical Paper 910180.

34. Naber, J.D. and Reitz, R.D.(1988), "Modeling Engine Spray/Wall Impingement", SAE Technical Paper 880107.

35. Wachters, L.H.J. and Westerling, N.A., " The Heat Transfer from a Hot Wall to Impinging Water Drops in the Spheroidal State," Chem. Eng. Sci. **21**, pp. 1047-1056, 1966.

Table 1. Gas-phase B.C. and droplet-phase I.C.

Air Mass Flow Rate	**355 kg/hr**
Air/Fuel Ratio	**20.17**
Inlet Air Temperature	**310 K**
Droplet Distribution	**Rosin-Rammler**
Sauter Mean Diameter	**127 μ m**
Droplet Size Range	**10 ~ 290**
Number of Size Range	**15**
Axial Droplet Velocity	**11 m/s**
Tangential Droplet Velocity	**6.1 m/s**
Radial Droplet Velocity	**0.5 ~ 2.5 m/s**
Droplet Temperature	**310 K**

Table 2. Test Conditions for the Measurement of Hiroyasu and Kadota

Nozzle diameter: 300 μm Injection Pressure: 9.9 MPa

Case	Pgas (MPa)	ρgas (kg/m^3)	Vinj (m/s)	$\dot{M}_{inj}$ (kg/s)	SMD (μm)
1	1.1	12.36	115.80	0.00688	42.4
2	3.0	33.70	102.54	0.00609	49.0
3	5.0	56.17	86.41	0.00513	58.8

Table 3. Test Conditions for the Measurement of Yokota et. al.

Case	Pinj (MPa)	Pgas (MPa)	Tamb (K)	Minj (kg/s)	Atmosphere
Evaporating Spray	30	3.0	900	0.00326	N_2
Burning Spray	30	3.0	900	0.00326	Air

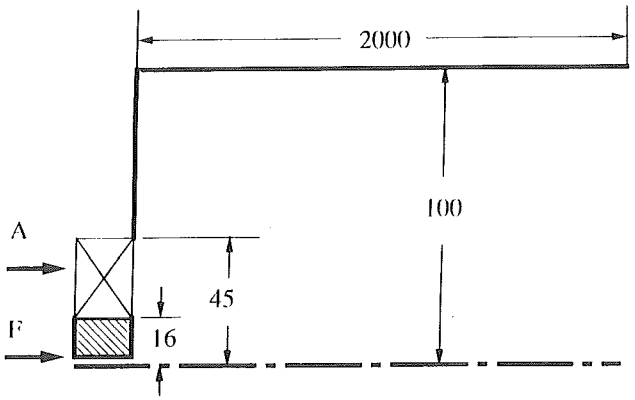

Figure 1 Geometry of the hollow-cone spray combustor(Khalil et. al.)

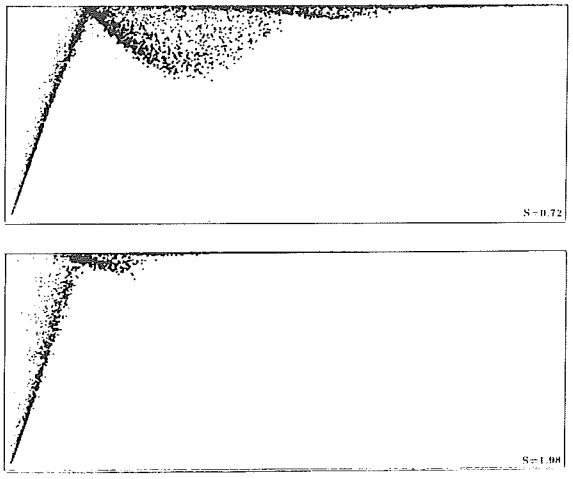

Figure 2 Droplet trajectories in kerosene spray flame fields

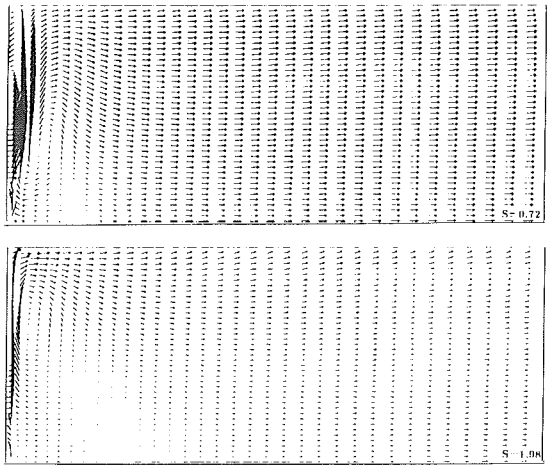

Figure 3 Velocity vectors in kerosene spray flame fields

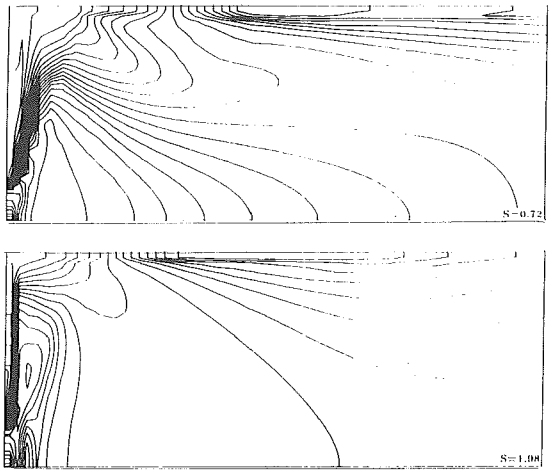

Figure 4 Temperature contours in kerosene spray flame fields

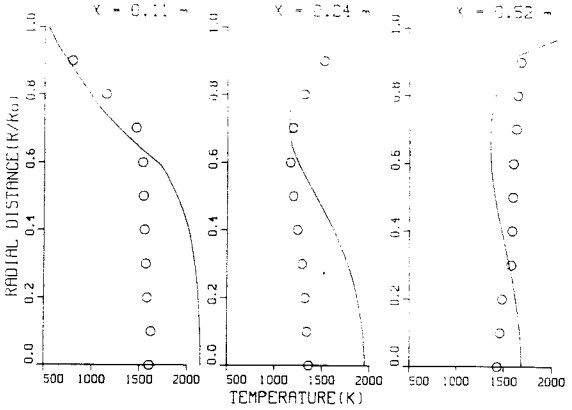

Figure 5 Radial profiles of mean temperature(S=0.72)

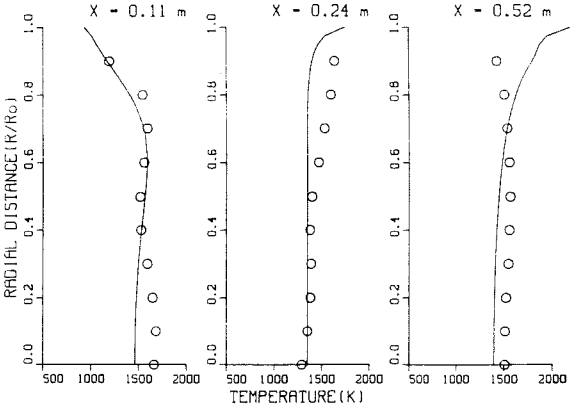

Figure 6 Radial profiles of mean temperature(S=1.98)

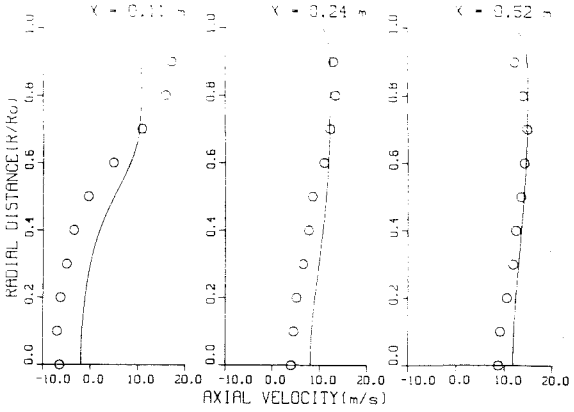

Figure 7 Radial profiles of mean axial velocity(S=0.72)

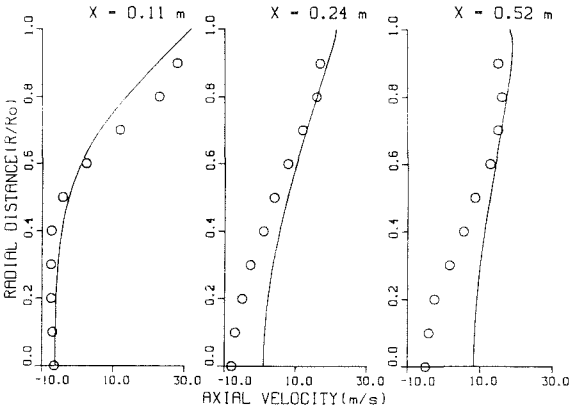

Figure 8 Radial profiles of mean axial velocity(S=1.98)

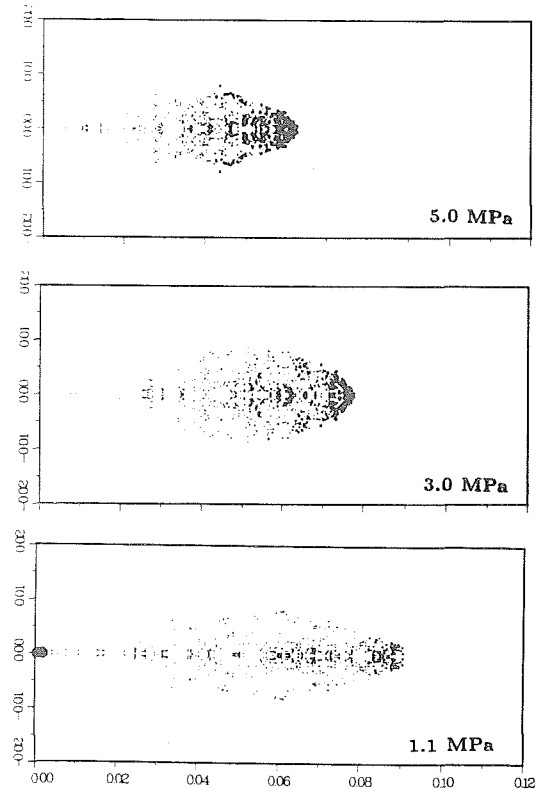

Figure 11 Spray parcel distribution in a solid-cone spray($t = 3.0ms$)

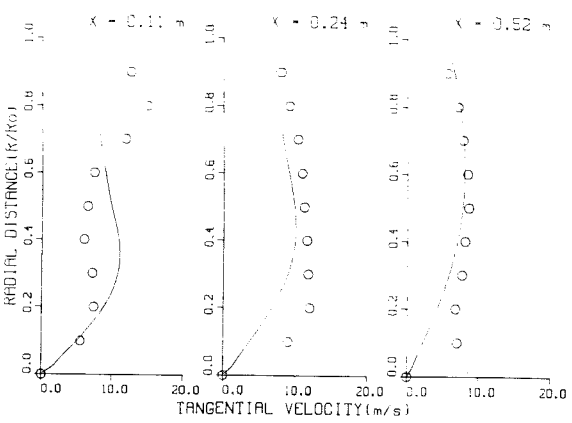

Figure 9 Radial profiles of mean tangential velocity(S=0.72)

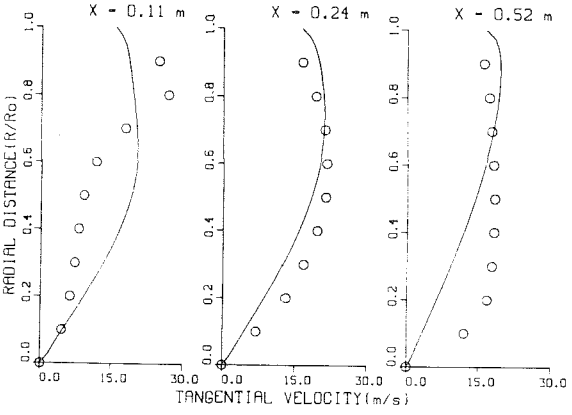

Figure 10 Radial profiles of mean tangential velocity(S=1.98)

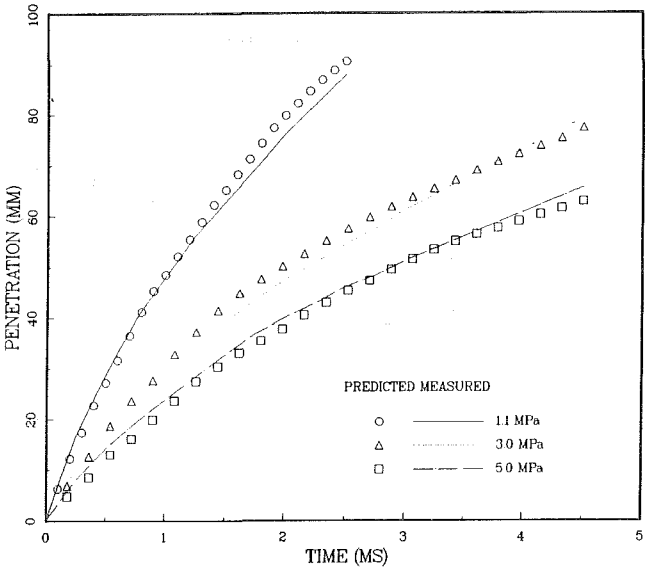

Figure 12 Spray tip penetration versus time in a solid-cone spray

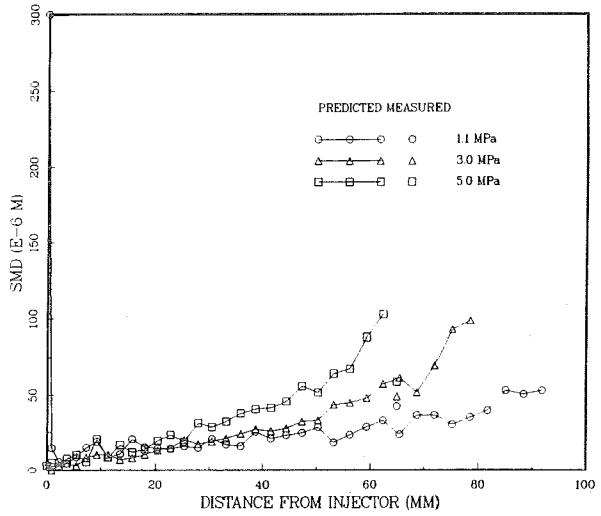

Figure 13 Sauter mean diameter versus distance from the injector

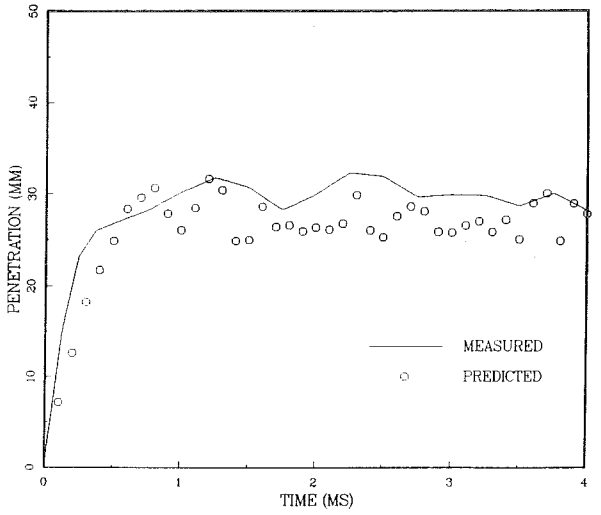

Figure 15 Spray tip penetration versus time in an evaporating spray

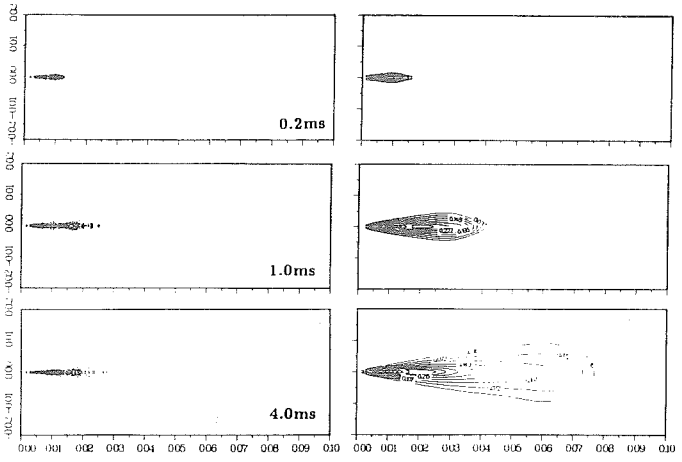

Figure 14 Spray parcel distribution and contours of fuel mass fraction in an evaporating spray

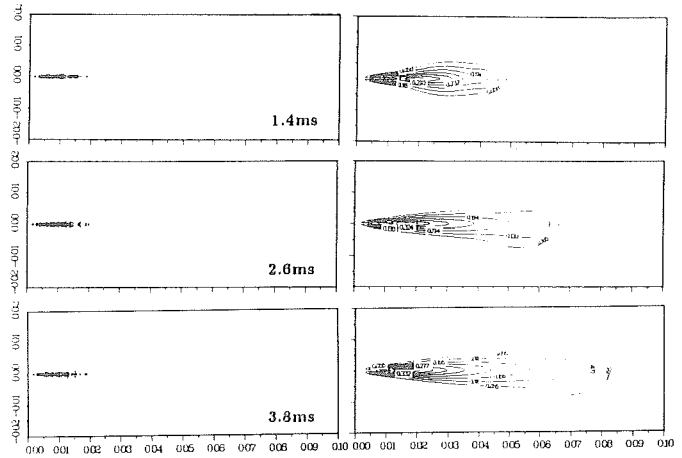

Figure 16 Spray parcel distribution and contours of fuel mass fraction in a burning spray

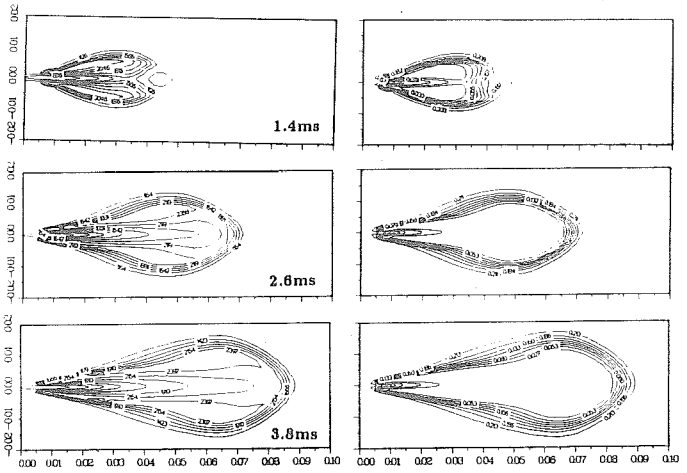

Figure 17 Contours of temperature and oxygen mass fraction in a burning spray